

Lightning Overvoltages in Windfarm considering Surge Characteristics of Grounding Resistance

S. Sekioka, K. Yamamoto, T. Funabashi

Abstract—A blade of wind turbine with a couple of MW has very tall height of more than one hundred meters. Lightning often strikes a receptor on blade. Lightning overvoltages due to a direct lightning strike to a wind power generation system cause damages in the system. Many parameters should be investigated to establish a rational lightning protection design for wind power generation system. Numerical simulation is a useful method to discuss the parameters. This paper uses Electro-Magnetic Transients Program (EMTP) for lightning surge analysis. This paper discusses the influence of transient response of grounding resistance on the lightning overvoltages in a wind power generation system for the direct lightning strike to the system.

Keywords: lightning overvoltage, wind power generation system, grounding resistance, transients.

I. INTRODUCTION

RENEWABLE energy sources are greatly expected to overcome global warming. Lightning protection for the renewable energy sources is a very important issue [1]. A wind tower for wind turbine with more than one megawatts is tall, and lightning frequently strikes wind power generation system. Many lightning-caused troubles have occurred in wind power generation systems [2, 3]. A lightning protection design based on lightning protection zone has been published [4]. A blade is the most important part in lightning protection for wind power generation system because it is exposed to lightning [3]. Thus, rational lightning protection design for wind power generation system should be established.

This paper discusses lightning overvoltages in underground cables in collector system of a windfarm. The authors have simulated lightning performance in the cables for some parameters such as cable sheath grounding and grounding resistance. Transient response of the grounding resistance affects the lightning overvoltages [5]. Thus, this paper carries out simulations for parameters of the grounding resistance model. This paper uses the EMTP [6] based on electrical circuit theory. The Finite-Difference Time-Domain (FDTD) method based on the electromagnetic field theory gives rigorous solution. Actual grounding system of a wind turbine

generation system is complicated because auxiliary grounding electrode such as counterpoise, ring electrode and vertical conductor are connector to tower base to obtain low grounding resistance. Rigorous surge response of complicated grounding system for lightning current can be obtained using the FDTD method [7]. The response is realized in the EMTP using fitting techniques and equivalent circuit [8]. Width of the sheath of cable is much thinner than the tower dimension. It is hard to simulate the lightning overvoltages in the cable using the FDTD method. Engineers require a simplified method to simulate various parameters to determine a grounding system. A vertical grounding conductor is often used as an auxiliary grounding electrode. This paper proposes formulas for surge characteristics of a vertical grounding conductor. An equivalent circuit of grounding system consists of resistors and an inductor. Therefore, this paper adopts the EMTP.

Vertical grounding rod is often used to obtain low low-frequency grounding resistance in Japan. This paper proposes formulas for constants of high-frequency grounding resistance. This paper discusses the influence of surge characteristics of grounding resistance on the lightning overvoltages in cables due to direct lightning strike to a wind power generation system. The constants of simulation models used in this paper are obtained using specifications of apparatuses and cables.

II. SURGE CHARACTERISTICS OF GROUNDING RESISTANCE OF WIND TURBINE

A. Lightning Surge Response of Grounding System

The high-frequency grounding resistance is not constant for high-frequency current such as lightning current. Fig. 1 shows equivalent circuit to represent the time dependence (inductive, flat and capacitive variations). The high-frequency grounding resistance in lightning surge analysis shows such the characteristics as frequency, time and current dependencies.

(1) Frequency dependence

The frequency dependence of high-frequency grounding resistance is caused by that of soil resistivity and permeability [9-10] as well as series impedance and shunt admittance even for constant soil parameters [11]. Alipio and Visacro proposed

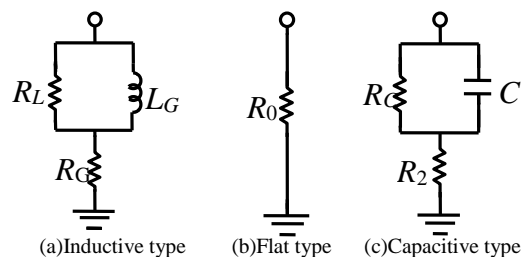


Fig. 1. Equivalent circuits of a grounding system.

S. Sekioka is with the Department of Electrical & Electronic Engineering, Shonan Institute of Technology, Fujisawa Japan (e-mail of corresponding author: sekioka@elec.shonan-it.ac.jp).

K. Yamamoto is with the Department of Electrical & Electronics Engineering, Chubu University, Kasugai, Japan (e-mail: kyamamoto@mem.iee.or.jp).

T. Funabashi is with the Electrical and Systems Engineering Program, Faculty of Engineering, University of the Ryukyus, Nishihara-cho, Japan (e-mail: h155869@tec.u-ryukyu.ac.jp).

$$\sigma_r(f) = 1 + A(f, \sigma_0) \quad (1)$$

$$\varepsilon_r(f) = \frac{\varepsilon'_\infty}{\varepsilon_0} + \frac{\tan(\pi\gamma/2) \times 10^{-3}}{2\pi f \varepsilon_0} \sigma_0 A(f, \sigma_0) \quad (2)$$

$$A(f, \sigma_0) = h(\sigma_0) \left(\frac{f[\text{Hz}]}{1\text{MHz}} \right)^\gamma$$

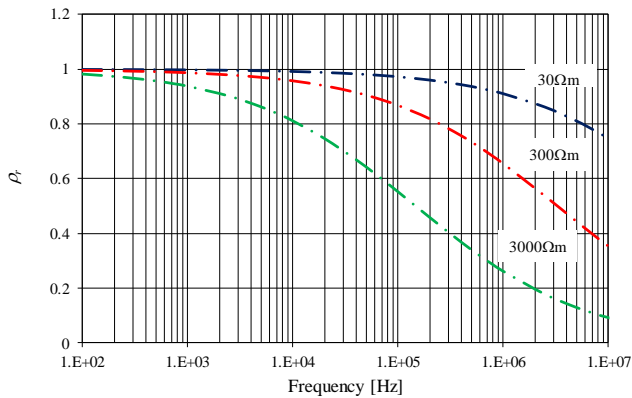
where $h(\sigma_0) = 1.26\sigma_0^{-0.73}$, $\gamma = 0.54$, $\varepsilon'_\infty/\varepsilon_0 = 12$, and $\sigma = \rho^{-1}$. the following empirical formulas for the frequency dependence of the soil relative resistivity and permittivity [10]. σ_0 is the low-frequency soil conductivity, and $\sigma_r = \sigma/\sigma_0$.

Fig. 2 shows the soil relative resistivity and permittivity using (1) and (2). The frequency dependence of the soil resistivity and permittivity greatly depend on the frequency. The frequency dependence of the high-frequency grounding resistance clearly appears for high grounding resistance [12].

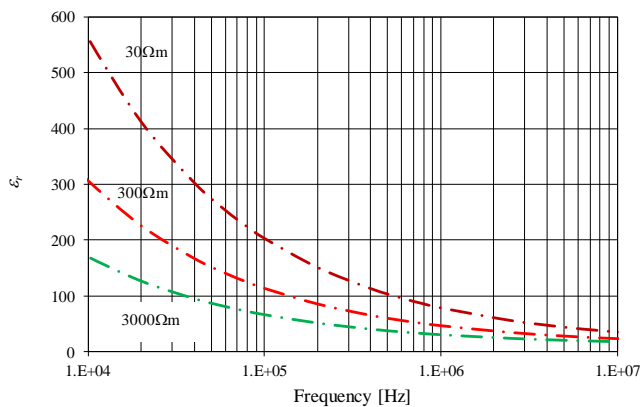
(2) Time dependence

A grounding electrode is a kind of grounding conductor. An L-type equivalent circuit of the grounding electrode is illustrated in Fig. 3.

The high-frequency grounding resistance converges to low-frequency grounding resistance. High low-frequency grounding resistance shows the capacitive variation. Low grounding resistance shows an inductive variation. The equivalent circuit suggests that the inductance is negligible for high low-frequency



(a)



(b)

Fig. 2. Frequency dependence of soil relative resistivity and permittivity (a) Soil relative resistivity (b) Soil relative permittivity.

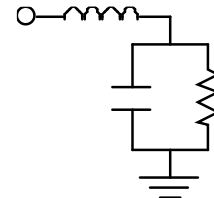


Fig. 3. An equivalent circuit of a grounding electrode.

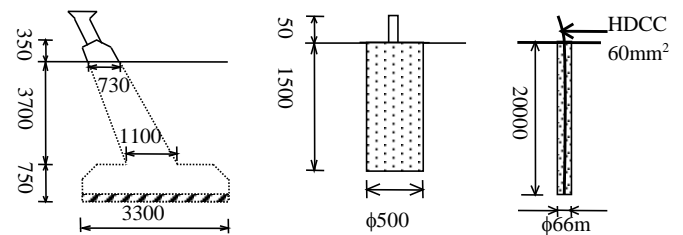
cy grounding resistance. However, the inductance of the high-frequency grounding resistance plays an important role for low low-frequency grounding resistance.

(3) Current dependence

Grounding resistance shows current dependence for high currents due to soil ionization. Figs. 4 and 5 show grounding electrodes for testing and measured results of the high-frequency grounding resistance [13-15]. The high-frequency grounding resistance for high current is estimated by V_m/I_m , where V_m is the crest value of applied voltage, and I_m is the crest value of applied current.

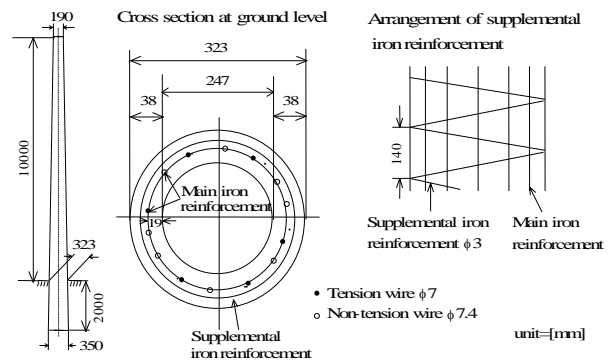
A low impulse-current generator (LIG) circuit of an impulse voltage generator [16] is different from a high-impulse current generator (HIG) circuit by the existence of a damping resistor. Waveforms of the applied currents are different. A grounding grid representing a 77kV substation grounding which is made of 60mm² HDCC wires and its burial depth is 1m (34m x 25m) is also examined. Experimental results of the grounding grid are included in Fig. 5(a). A part of the concrete pole in the ground is a kind of a grounding electrode [17].

Fig. 5(a) suggests the current dependence of the high-frequency grounding resistance is not clearly observed for large grounding electrodes. Fig. 5(b) indicates that the higher the soil resistivity, the heavier the current dependence of the high-frequency grounding resistance. The influence of the soil



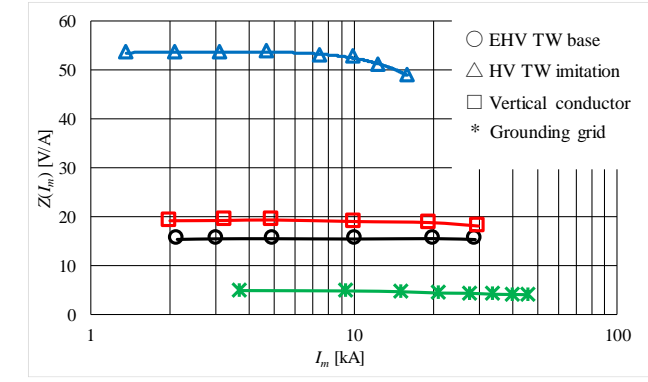
(a) EHV tower base

(b) HV imitation (c) Long vertical conductor

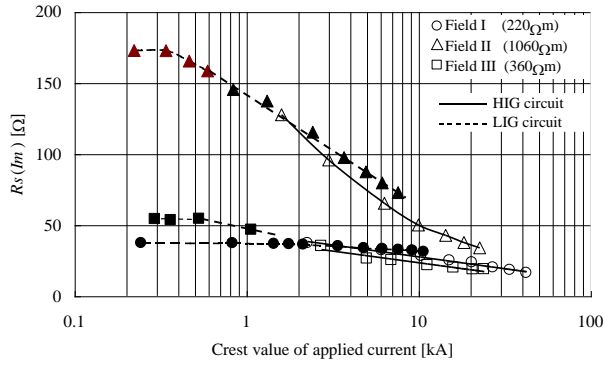


(d) Reinforced concrete pole

Fig. 4. Grounding electrodes for testing.



(a)



(b)

Fig. 5. Measured current-dependent high-frequency grounding resistance (a) Large grounding electrode (b) Reinforced concrete pole in different yards.

resistivity on the current dependence is observed for low currents of less than 10 kA. However, the difference of the grounding resistance decreases as the crest applied current increases. The high-frequency grounding resistance converges nearly to the value in the range of a few ten kiloAmps.

Wherever current density branching off through an electrode exceeds a critical value, the soil ionization occurs. The soil ionization zone of which the resistivity is much lower than the initial soil resistivity grows as the injected current increases. A relation between the soil ionization onset current I_c and the soil ionization gradient E_c [V/m] at a point on the contour of the ionization zone is given by:

$$I_c = E_c \frac{S_0}{\rho_0} \quad (3)$$

where ρ_0 is the soil resistivity with no soil ionization [Ωm], S_0 is the surface area of the electrode [m^2], and E_c is the soil ionization onset gradient.

Equation (3) indicates much high current is necessary for a large grounding electrode to cause the soil ionization. The measurement results in Fig. 5(a) suggests more than several tens kilo-amperes is needed for grounding resistance to be clearly decreased. Therefore, it is not necessary to consider the current dependence of the grounding resistance of wind power generation system because of large grounding electrode to obtain very low grounding resistance.

B. Simulation Model of Grounding System

Many formulas for low-frequency grounding resistance have been proposed. Dwight's formula [18] is well-known. (4)

is accurate expression of Dwight's formula. (5) is approximate formula for $l \gg r$. Liew-Darveniza's formula (6) is another formula, which is often used for the soil ionization [19].

$$R_G = \frac{\rho_0}{2\pi l} \left(\ln \frac{2l + \sqrt{r_0^2 + 4l^2}}{r_0} + \frac{r_0}{2l} - \sqrt{1 + \frac{r_0^2}{4l^2}} \right) \quad (4)$$

$$R_G = \frac{\rho_0}{2\pi l} \left(\ln \frac{4l}{r_0} - 1 \right) \quad (5)$$

$$R_G = \frac{\rho_0}{2\pi l} \ln \left(1 + \frac{l}{r_0} \right) \quad (6)$$

where r_0 is the electrode radius, and l is the electrode length.

Fig. 6 shows a comparison of $R_G/(\rho_0/2\pi l)$ of the formulas for low-frequency grounding resistance.

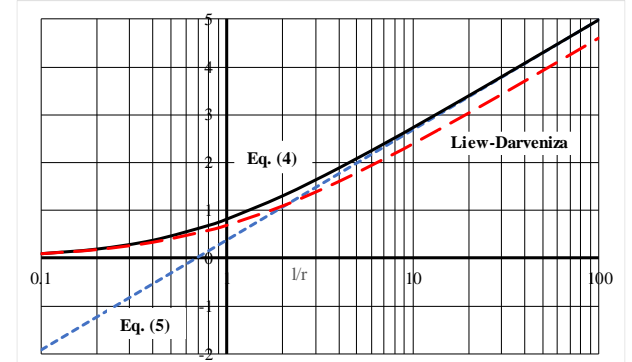


Fig. 6. Comparison of formulas for low-frequency grounding resistance of vertical grounding rod.

From Fig. 6, (6) gives sufficient accuracy in rough estimation of low-frequency grounding resistance. Considering tower base of wind tower which is not satisfied with $l \gg r$, (6) is convenient.

Considering image in the air, an inductance of a vertical grounding rod is given by [20]

$$L_G = \frac{60l}{v_0} \left(\ln \frac{2l + \sqrt{r_0^2 + 4l^2}}{r_0} + \frac{r_0}{2l} - \sqrt{1 + \frac{r_0^2}{4l^2}} \right) \quad (7)$$

The low-frequency grounding resistance of wind power generation system in Japan is less than two ohms. Fig. 1(a) is used for an equivalent circuit of the wind power generation system.

Formulas for the high-frequency grounding resistance mentioned above is obtained assuming rod electrode. The grounding system of wind power generation system is complicated. Accurate values should be estimated using tools such as the FDTD method [21] and another technique based on the electromagnetic field theory.

Equations (4) and (7) give the following relation between the resistance and the inductance of vertical grounding rod.

$$L_G = \frac{120\pi}{v_0} l^2 \frac{R_G}{\rho_0} \quad (8)$$

The high-frequency grounding resistance model in Fig. 3 is very simple. Considering the low-frequency grounding resistance of the wind turbine grounding system is very low, the capacitor is negligible. R - L series circuit is a convenient model.

However, it has a disadvantage for very high frequency current because extremely high voltage appears. Therefore, a parallel resistor is necessary as shown in Fig. 1(a). The resistance R_G and inductance L are given by (4) to (6) and (7), respectively. R_L is the initial value of the high-frequency grounding resistance. The surge impedance of conductor is adopted as R_L . The surge impedance is given by

$$R_L = v \frac{L}{l} \quad (9)$$

where v is the surge velocity on the grounding conductor.

$$\frac{R_L}{L/T_f} = \frac{vL/l}{L/T_f} = \frac{vT_f}{l} \quad (10)$$

where T_f is the rise time of injection current.

If vT_f is not much longer than l , R_L should not be ignored.

As an example, measured result of grounding system of a wind power generation system in [21] is discussed. The grounding system consists of a tower base with length of 2m and radius of about 4.8m, and vertical rods with 50m. Measured low-frequency grounding resistance is $R_G = 0.062\Omega$. $v = 100\text{m}/\mu\text{s}$ is used. This value is frequently observed. (8) and (9) give $L = 14.0\mu\text{H}$ and $R_L = 26.9\Omega$. Reference [5] estimates the constants of the grounding resistance model to be $R_L = 10\Omega$ and $L = 5.2\mu\text{H}$ from the measured step response. (8) gives relatively large value in comparison with the measured result. $L = 5.2\mu\text{H}$ gives $R_L = 10\Omega$. Considering (8) and (9) are very simple, (8) and (9) are convenient.

III. SIMULATION CIRCUIT

A. Wind Power Generation System for Simulation

Fig.7 illustrates a wind power generation system to estimate lightning overvoltages. Wind turbines are connected to a

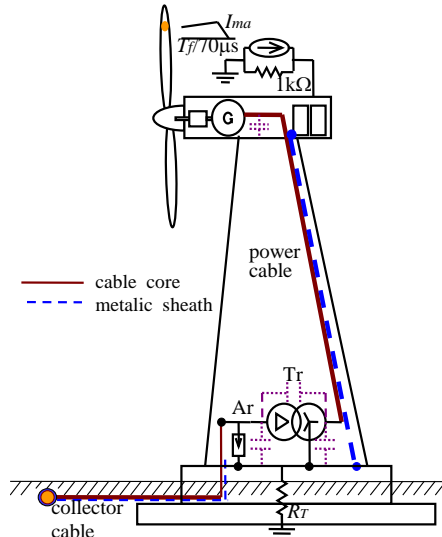


Fig. 7. Wind power generation system.

TABLE I. SPECIFICATIONS OF GENERATOR AND TRANSFORMER

Connection method	Y-Δ
Rated power of generator	1.5 MVA
Rated voltage of transformer	690/22,000 V
Power frequency	50 Hz
% impedance of transformer	6 %

substation. The specifications of a generator and a transformer are shown in Table I [22]. The neutral terminal of the transformer is directly connected to the tower base. Under-ground cable in collection system and power cable in tower are 22kV CVT 200mm² and CV 200mm², respectively.

B. Simulation Models

Simulation models of tower, transformer and generator are same as those in reference [5].

1) Power Line

This paper uses the Semlyen model [23] for the collector cables. Cable constants are estimated using an EMTP support program "CABLE PARAMETERS" [24]. The cable in the collector system is terminated by characteristic impedance matrix as a matching circuit at an end of the line to represent a long line [25]. The collector cable has a twisted configuration and can be treated as a transposed line. Maximum observation time in this paper is 50μs. This period approximately corresponds to 20kHz, which higher than critical frequency of the collector cable. The transformation matrix in modal domain can be regarded to be independent of frequency [26].

3) Grounding System

The low low-frequency grounding resistance shows inductive variation [21]. This paper uses the equivalent circuit of Fig. 1(a). The soil resistivity for estimating the constants of underground cables assumes 300Ωm.

4) Surge Arrester

Surge arrester is represented by piecewise-linearly-varying resistance, which is given by current-voltage characteristics shown in Fig. 8.

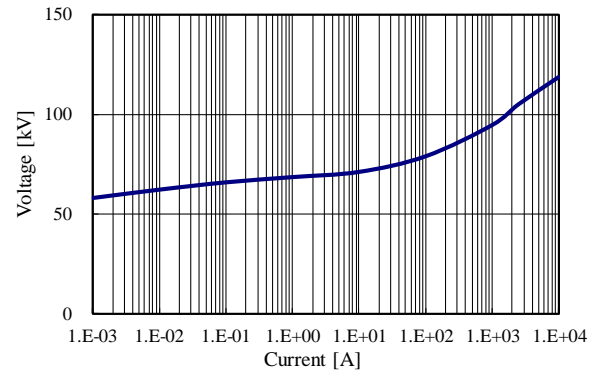


Fig. 8. Voltage - current curve of arrester.

5) Lightning Current

Lightning current waveform is assumed to be triangle shape of 2/70μs. The lightning is represented by a current source and a lightning channel impedance of 1kΩ [27]. Polarity of lightning current in the simulations is assumed to be positive.

IV. SIMULATION RESULTS

A. Simulation Cases

Metallic sheath of collector cable should be grounded for lightning protection. Grounding of both the terminals of the sheath causes power loss, and an end of the sheath is sometimes opened. This paper assumes P/S side of the cable is grounded, and the other side is opened.

Cable length is assumed 100m. Lightning strike to TW1 which is located at the end of the windfarm as in Fig. 9. Lightning often strikes the end of the windfarm considering the relation between the wind towers and the direction of cloud [28]. Peak value of lightning current is assumed 26kA. This value is 50% value of cumulative frequency distributions of peak lightning current [29].

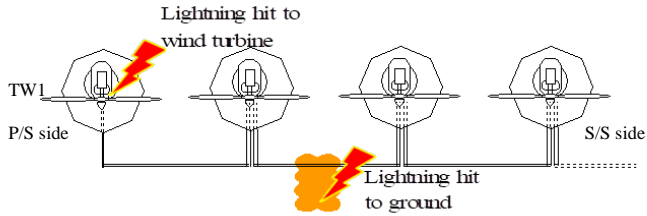


Fig. 9. Lightning events in a windfarm.

B. Constants of Grounding Resistance Model

A tower base with radius of 4.8m and length of 2m is chosen for discussion. Fig. 10 shows the constants of the grounding resistance model in Fig. 1(a) as a parameter of the soil resistivity. The inductance L_G and resistance R_L to represent the inductive variation are independent of the soil resistivity, and the low-frequency grounding resistance R_G is proportional to the soil resistivity because the dimension of the grounding electrode is fixed.

The grounding electrode is taken to be long to obtain low grounding resistance. Fig. 11(a) shows the length as a parameter of soil resistivity so that the low-frequency grounding resistance is two ohms. Fig. 11(b) shows the constants of the grounding resistance model.

C. Influence of Grounding Resistance on Lightning Overvoltages in Collector Cable

Fig. 12 shows peak value of the cable core potential and the core voltage to the tower base for the lightning strike to TW1 as a parameter of the soil resistivity. The dimensions of the grounding electrode of the wind tower are $r=4.8\text{m}$ and $l=2\text{m}$. The constants of the grounding resistance model are obtained from Fig. 10. From Fig. 12(a), the voltages become higher as the soil resistivity is higher. On the other hand, the core voltage to the tower base is saturated for high soil resistivity. Considering the arrester voltage at one ampere is about 70kV, the voltage is suppressed by the surge arrester for high soil resistivity.

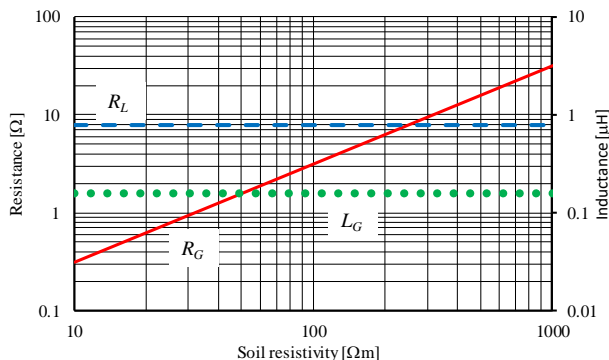
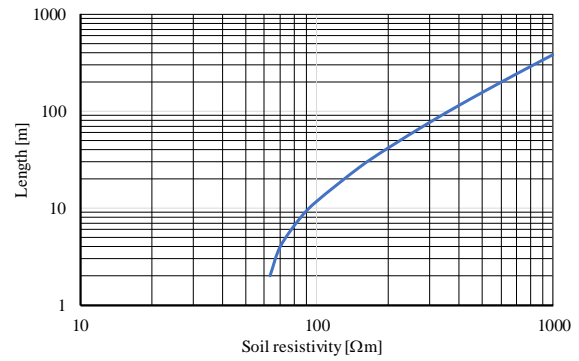
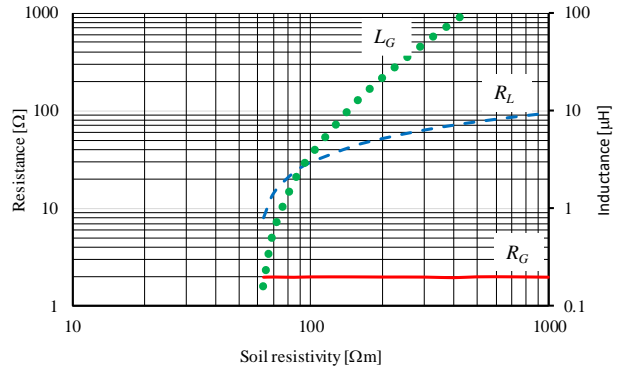


Fig. 10. Constants of grounding resistance model as a parameter of soil resistivity.

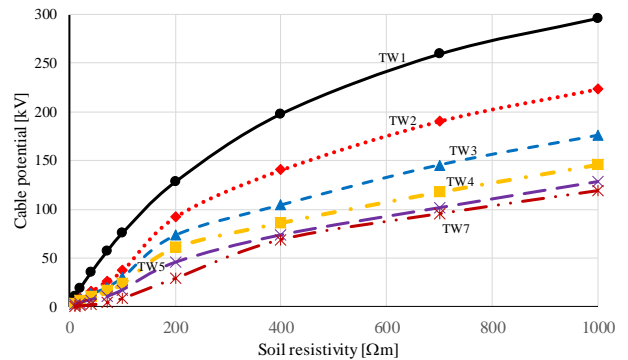


(a)

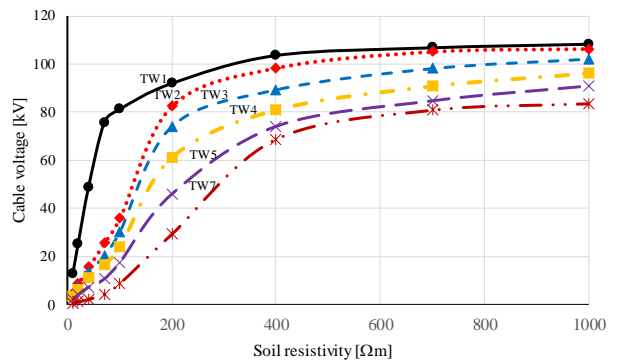


(b)

Fig. 11. Constants of grounding resistance model so that low-frequency stance is two Ohms. (a) Length (b) Constants of grounding resistance model.



(a)



(b)

Fig. 12. Peak value of core potential and core voltage to tower base as a parameter of soil resistivity. (a) Core potential (b) Core voltage to tower base.

Fig. 13 shows peak value of the core potential and the core voltage to the tower base for the lightning strike to TW1 as a parameter of soil resistivity. The low-frequency grounding

resistance is two ohms. The constants of the grounding resistance model are obtained from Fig. 11. The low-frequency grounding resistance is independent of the soil resistivity. Therefore, the soil resistivity dependence of the voltage is caused by the influence of the inductance. Thus, the transient response of the grounding resistance is important for lightning surge analysis. The core voltage to the tower base at the lightning striking tower is high for relatively low soil resistivity. Thus, the transient response of grounding resistance is very important.

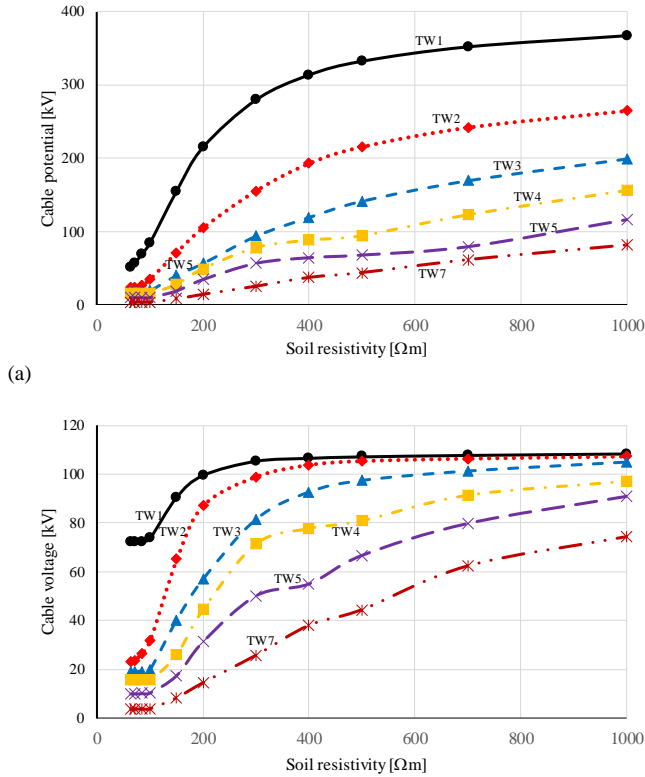


Fig. 13. Peak value of core potential and core voltage to tower base as a parameter of soil resistivity in case that low-frequency grounding resistance is fixed. (a) Core potential (b) Core voltage to tower grounding.

V. CONCLUSION

This paper has discussed lightning overvoltages in underground cable in collector system of a windfarm for direct lightning strike to a receptor. The simulation results show that the transient response of grounding resistance greatly affects the cable voltages. The transient response should be considered for accurate lightning surge analysis of wind power generation system.

VI. REFERENCES

- [1] T. Funabashi edit., Integration of Distributed Energy Resources in Power Systems – Implementation, Operation, and Control –, Academic Press, 2016.
- [2] NEDO, Report on study of lightning protection measures for wind turbine generator system, 2013 (in Japanese).
- [3] CIGRE WG C4.409, “Lightning protection of wind turbine blades,” *CIGRE Technical Brochure* no. 578, 2014.
- [4] IEC 61400-24, Wind Turbines-Part 24: Lightning protection, 2010.

- [5] S. Sekioka, H. Otaguro, and T. Funabashi, “A study on overvoltages in windfarm caused by direct lightning stroke,” *IEEE Trans. on Power Delivery*, to be published, 2019.
- [6] W. S. Meyer: “ATP Rule Book”, BPA, 1984.
- [7] K. Tanabe, “Novel method for analyzing dynamic behavior of grounding systems based on the finite-difference time-domain method,” *IEEE Power Engineering Review*, pp. 55-57, 2001.
- [8] A. De Conti, and R. Alipio, “Single-port equivalent circuit representation of grounding systems based on impedance fitting,” *IEEE Trans. Electromagn. Compat.* to be published, 2019.
- [9] S. Visacro, and R. Alipio, “Frequency dependence of soil parameters: experimental results, predicting formula and influence on the lightning response of grounding electrodes,” *ibid. Power Del.*, vol. 27, no. 2, pp. 927-935, 2012.
- [10] R. Alipio, and S.Visacro, “Modeling the frequency dependence of electrical parameters of soil,” *ibid. Electromagn. Compat.*, vol. 56, no. 5, pp. 1163-1171, 2014.
- [11] N. Theethayi, R. Thottappillil, M. Paolone, C.A.Nucci, and F. Rachidi, “External impedance and admittance of buried horizontal wires for transient studies using transmission line analysis,” *IEEE Trans., Dielectrics & Electrical Insulation*, vol. 14, no. 3, pp. 751-761, June, 2007.
- [12] S. Sekioka, “Frequency and current dependent grounding resistance model for lightning surge analysis,” *ibid. Electromagn. Compat.*, vol. 61, no. 2, pp. 419-425, 2019.
- [13] S. Sekioka, H. Hayashida, T. Hara, and A. Ametani, “Measurements of grounding resistances for high impulse currents,” *IEE Proc. of Gener., Transm. & Distrib.*, vol. 145, no. 6, pp. 693-699, 1998.
- [14] S. Sekioka, T. Sonoda, and A. Ametani, “Experimental study of current-dependent grounding resistances of rod electrode,” *IEEE Trans. Power Delivery*, vol. 20, no. 2, pp. 1569-1576, 2005.
- [15] A. Morimoto, H. Hayashida, S. Sekioka, M. Isokawa, T. Hiyama, and H. Mori, “Development of weather proof mobile impulse voltage generator and its application to experiments on nonlinearity of grounding resistances,” *Trans. of Electrical Engineering in Japan*, vol. 117, no. 5, pp. 22-33, 1997.
- [16] T. Matsui, M. Adachi, H. Fukuzono, S. Sekioka, O. Yamamoto, and T. Hara, “Measurements of grounding resistances of a transmission-line tower base connected with auxiliary grounding electrodes for high impulse currents,” in *Proc. 10th Int. Symp. on High Voltage Engineering*, vol. 5, pp. 257-260, Montreal, Canada, 1997.
- [17] S. Sekioka, “Lightning surge analysis model of reinforced concrete pole and grounding lead conductor in distribution line”, *IEEJ Trans. Electrical and Electronic Engineering*, vol. 3, pp. 432-440, 2008.
- [18] H. B. Dwight, “Calculation of resistances to ground,” *Electrical Engineering*, vol. 55, pp. 1319-1328, 1936.
- [19] A. C. Liew, and M. Darveniza, “Dynamic model of impulse characteristics of concentrated earth,” *Proc. IEE*, vol. 121, pp. 123-135, 1974.
- [20] K. Okumura, and A. Kishima, “A method for computing surge impedance of transmission line tower by electromagnetic field theory,” *Trans. IEE of Japan*, vol. B-105, no. 9, pp. 733-740, 1985.
- [21] K. Yamamoto, S. Yanagawa, K. Yamabuki, S. Sekioka, and S. Yokoyama, “Analytical surveys of transient and frequency-dependent grounding characteristics of a wind turbine generator system on the basis of field tests,” *IEEE Trans. Power Del.*, vol. 25, no. 4, pp. 3035- 3043, 2010.
- [22] www.jstage.jst.go.jp/article/jwea/33/1/33_25/_pdf (in Japanese)
- [23] A. Semlyen and A. Dableanu, “Fast accurate switching transient calculations transmission lines with ground return using recursive convolutions”, *ibid. Power App. Syst.*, vol. 94, no. 2, pp. 561-571, 1975.
- [24] A. Ametani: Cable Parameters Rule Book, Japanese EMTP committee, 1996.
- [25] A. Ametani, and T. Kawamura, “A method of a lightning surge analysis recommended in Japan using EMTP,” *IEEE Trans., Power Del.*, vol. 20, no. 2, pp. 867-875, 2005.
- [26] A. Ametani, Distributed-Parameter Circuit Theory. *Corona Pub.*, Tokyo, 1990 (in Japanese).
- [27] V. Rakov, and M. A. Uman, LIGHTNING – Physics and effects -, Cambridge University Press, 2003.
- [28] T. Sakata, K. Yamamoto, S. Sekioka, and S. Yokoyama, “Lightning protection effect of lightning tower set up in wind power station based on upward leader progression model”, *Trans. IEE of Japan*, vol. 131, no. 2, pp. 215-221, 2011 (in Japanese).
- [29] CRIEPI Sectional Committee for Transmission Lines, Lightning Protection Design Study Committee, “Lightning proof design guide-book for transmission lines”, *CRIEPI Report*, no.175031, 1976 (in Japanese).